IEEE Access
Multidisciplinary | Rapid Review | Open Access Journal

IEEE ENGINEERING IN MEDICINE AND BIOLOGY SOCIETY SECTION

Received 24 March 2023, accepted 19 April 2023, date of publication 24 April 2023, date of current version 2 May 2023.

*Digital Object Identifier 10.1109/ACCESS.2023.3269596*

RESEARCH ARTICLE

# High-Fidelity Compressive Heart Rate Tracking

**SEUNGYOON NAM[1,2], CHANKI PARK[2], AND HYUNSOON SHIN[1,2,3]**
[1]Department of Computer Software, ICT, University of Science and Technology, Yuseong-gu, Daejeon 34113, South Korea
[2]Electronics and Telecommunications Research Institute, Yuseong-gu, Daejeon 34129, South Korea
[3]Emotion Information Communication Technology Industrial Association, Daejeon 34129, South Korea

Corresponding authors: Chanki Park (chanki@etri.re.kr) and Hyunsoon Shin (hsshin@etri.re.kr)

This work was supported by the Industrial Technology Innovation Program, Development of Emotional Cognitive and Sympathetic AI Service Technology for Remote (Non-face-to-face) Learning and Industrial Sites, funded by the Ministry of Trade, Industry and Energy (MOTIE), South Korea, under Grant 20012603.

**ABSTRACT** Recently, photoplethysmography sensors in smart watches have been frequently used to monitor heart rate. Because a photoplethysmography sensor flashes light on the skin and measures the reflected light, the rate of flashing and sampling is directly related to its energy consumption. It is necessary to reduce the rate to extend the battery life of a smart watch. In this study, to satisfy sub-Nyquist sampling, real-time, and high accuracy requirements, we propose a novel heart rate tracking method that consists of online compressive covariance sensing, signal subspace tracking, and spectral peak tracking. The proposed method (average sampling rate: 1.4 Hz) showed better frequency tracking performance than the conventional spectral peak tracking algorithm (sampling rate: 10 Hz) in time-varying heart rate simulations, and a statistically significant difference between them was not observed in the real photoplethysmogram data. The trimmed average absolute error was 1.04 beats/min. As a result, the proposed real-time heart rate tracking method with sub-Nyquist sampling showed high accuracy.

**INDEX TERMS** Heart rate, photoplethysmogram, sub-Nyquist sampling, subspace tracking, spectral peak tracking.

## I. INTRODUCTION

With a growing population of cardiovascular disease, heart rate (HR) monitoring is a crucial consideration in mobile healthcare. Several factors cause changes in HR, such as physical activity, autonomic nervous system, body metabolism, age, venous return, and body size [1]. Recent advances in smart watches with photoplethysmography sensors have made it possible to track the HR throughout the day. The photoplethysmography sensor measures changes in the blood volume, and its frequency analysis is used for instantaneous HR estimation [2].

Various algorithms have been developed for instantaneous frequency estimation. Empirical mode decomposition [3], wavelet transform [4], Wigner-Ville distribution [5], and synchrosqueezing transform [6] allow efficient time-frequency analysis, but are not suitable for real-time HR tracking. Among the various instantaneous frequency estimators, an adaptive lattice notch filter (ALNF) has been used to estimate the instantaneous HR and respiratory rate from photoplethysmogram (PPG) with high accuracy and low computational complexity [7], [8], [9]. To track the HR from PPG contaminated by motion artifacts, Jhang et al. proposed the TROIKA framework [10], which has been utilized in many recent studies. In the TROIKA framework, a singular spectrum analysis is employed to extract a clean PPG, and the instantaneous HR is then estimated by spectral peak tracking (SPT) consisting of 1) initialization, 2) peak selection, and 3) validation. The former step can be interpreted as a type of signal subspace estimation, which is broadly used to improve spectral accuracy [11], [12]. As a PPG filtering step, multiple measurement vector model [13], adaptive filters [14], [15], and ensemble empirical mode decomposition [16] have been utilized, and multiple initialization SPT [17] and finite state machine scheme [18] have been designed to improve the HR tracking step.

Because the photoplethysmography sensor has a LED that needs to flash at sampling instants, the rate of LED flashing

The associate editor coordinating the review of this manuscript and approving it for publication was Carmen C. Y. Poon.

and sampling is directly related to the energy consumption of the smart watch [19]. It is important to reduce this rate to extend the battery life of smart watches and bands. Compressed sensing is well known technique to recover the original signal from fewer samples than the Nyquist sampling rate, but it cannot lower the LED flashing rate because it demands a whole analog signal [20], [21], [22]. On the other hand, sub-Nyquist sampling techniques such as nested sampling [23], [24], [25], coprime sampling [26] and compressive covariance sensing (CCS) [27], [28], [29] can reduce the LED blinking rate as well as the sampling rate. The sub-Nyquist sampling technique samples a signal at patterned timing and reconstructs the covariance instead of signal itself. Among sub-Nyquist sampling techniques, nested sampling has redundant samples, and coprime sampling contains holes in the covariance [24]. However, compressive covariance sensing (CCS) [27], [28], [29] can achieve minimum redundant sampling without holes in the covariance. Moreover, the online version of CCS can handle non-stationary signals (e.g., time-varying HR) [30].

An online CCS-based HR tracking method was proposed in [19]. An adaptive covariance notch filter (ACNF) was proposed to estimate HR from the covariance of PPG, but its HR tracking performance was insufficient. To improve the estimation accuracy, several subspace methods based on a covariance matrix, such as Multiple Signal Classification (MUSIC) and Blackman-Tukey method, have been developed [31]. These algorithms demanded signal and noise subspaces, but there was no algorithm to track these subspaces with only the covariance without using the original signal. In this study, to achieve high-fidelity frequency tracking, a signal subspace tracking (SST) algorithm based on a covariance matrix was designed. Finally, we propose a novel HR tracking method that combines online CCS, SST, and SPT to satisfy real-time processing, energy-efficient sampling, and high accuracy. The proposed method is described in Section II. In Section III, the HR tracking performance is assessed using simulations and real PPG data. The results are interpreted and discussed in Section IV. Finally, Section V concludes the study.

## II. METHODS

The maximum HRs for normal adults are less than 3.5 Hz [32], [33], but may exceed in some patients [34], [35], [36], [37], [38]. Moreover, since the HR is an average value within a time window, the instantaneous HR can be higher than the HR. In this study, we consider the upper limit of instantaneous HR as 5 Hz and its Nyquist rate as 10 Hz. Sub-Nyquist sampling is the only way to reduce the rate for sampling and LED flashing of a photoplethysmography sensor. In this study, we propose a novel HR tracking algorithm that consists of online CCS, SST, and SPT to satisfy both sub-Nyquist sampling and high accuracy (see Fig. 1).

### A. ONLINE COMPRESSIVE COVARIANCE SENSING

Online CCS consists of compression and recovery steps. In the compression step, online CCS utilizes a circular sparse ruler (CSR) as the sampling pattern. A CSR has a higher compressibility than a linear sparse ruler [29]. A CSR of length (N-1) has M marks, which are integers between 0 and N-1. For all integers $l$ from 0 to N-1, the CSR must have at least one pair of marks (m and m′) such that

$$(\mathrm{m} - \mathrm{m}')\%\mathrm{N} = l \tag{1}$$

where % means the modulo operator, and (1) represents the distance $l$ between two marks m and m' of a CSR. The compression ratio corresponds to M/N. A CSR with a long length of (L-1) can be designed (L = N × B) by concatenating the same B CSRs. In this study, we designed a CSR with N = 57, M = 8, and B = 4, as illustrated in Fig. 2. Online CCS samples the original signal with a CSR pattern and stores the samples and their marks in a two-dimensional queue. In the recovery step, the online CCS reconstructs the length L covariance vector from the two-dimensional queue, and the recovery algorithm is described in Algorithm 1.

In Algorithm 1, $\eta$ is the forgetting factor ($0 \leq \eta < 1$), which is the parameter of the exponentially weighted moving average; a high $\eta$ leads to high accuracy but low convergence speed. Hence, it is necessary to adjust $\eta$ according to the degree of non-stationarity. For example, when HR varies dynamically, $\eta$ should be low; however, a high $\eta$ is suitable for estimating static HR. Because filtering must be performed after the covariance recovery step of the online CCS, we filtered a covariance vector using a 5$^{\text{th}}$ order Butterworth bandpass filter (0.7–3 Hz) as covariance filtering [19].

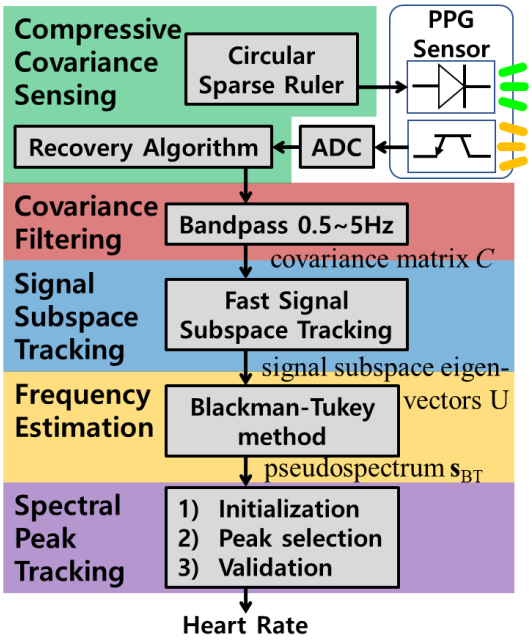


**FIGURE 1.** Block diagram of the proposed heart rate tracking method.

### B. COMPRESSIVE SPECTRAL PEAK TRACKING

The HR can be estimated from the covariance of PPG because the Fourier transform of the covariance vector is a power

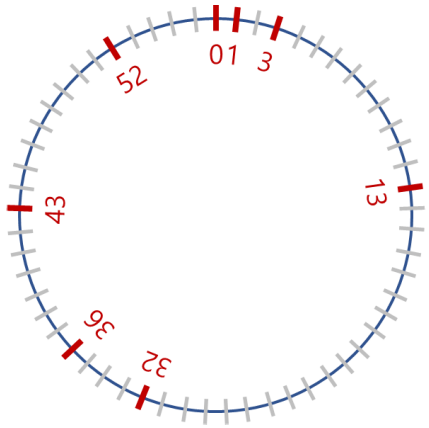


**FIGURE 2.** Circular sparse ruler of length 56. (N = 57, M = 8).

**Algorithm 1** Covariance Recovery of Online CCS

**Input:** Sample $x$ and its mark $i$ at iteration $k$
**Output:** Recovered covariance vector $\boldsymbol{c}_k$ at iteration $k$

$\boldsymbol{c}_k = \boldsymbol{c}_{k-1}$
$\boldsymbol{x}_k = [x, \boldsymbol{x}_k(1),\ldots, \boldsymbol{x}_k(\mathrm{M{\cdot}B\text{-}1})]$
$\boldsymbol{i}_k = [i, \boldsymbol{i}_k(1),\ldots, \boldsymbol{i}_k(\mathrm{M{\cdot}B\text{-}1})]$
**for** b = 0:B-1
  **for** m = 1:M
    $l = (\boldsymbol{i}_k(\mathrm{m{+}M{\cdot}b})\text{-}i)\%\ \mathrm{N{+}N{\cdot}b}$
    $\boldsymbol{c}_k(l) = \eta{\cdot}\boldsymbol{c}_k(l){+}(1\text{-}\eta)\cdot x{\cdot}\boldsymbol{x}_k(\mathrm{m{+}M{\cdot}b})$
  **end**
**end**

* %: modulo operator

spectrum of PPG. To focus on the HR range (0.7–3 Hz), we define a partial discrete Fourier transform matrix F as follows:

$$F = \begin{bmatrix} e^{-j2\pi k_1 \frac{0}{L}} & \cdots & e^{-j2\pi k_1 \frac{L}{L}} \\ \vdots & \ddots & \vdots \\ e^{-j2\pi k_2 \frac{0}{L}} & \cdots & e^{-j2\pi k_2 \frac{L}{L}} \end{bmatrix}, \begin{cases} k_1 = round(L\frac{0.7}{fs/2}) \\ k_2 = round(L\frac{3}{fs/2}) \end{cases} \tag{2}$$

where $fs$ is the sampling frequency and round() returns the nearest integer. The frequency bin $\mathbf{s}$ for the HR is expressed as follows:

$$\mathbf{s} = \mathrm{F}\,\boldsymbol{c}_k \tag{3}$$

where $\boldsymbol{c}_k$ is a covariance vector reconstructed using online CCS. To ensure the stability of HR tracking, we smoothed $\mathbf{s}$ as follows:

$$\mathbf{s}_{\mathrm{PS}} = \gamma \cdot \mathbf{s}_{\mathrm{PS}} + (1-\gamma)\cdot \mathbf{s} \tag{4}$$

where $\gamma$ is the smoothing factor ($0 \le \gamma < 1$). Based on the power spectrum $\mathbf{s}_{\mathrm{PS}}$, the instantaneous HR is estimated using SPT [10]. We denote this method as "CCS+SPT". Because of the convergence time of online CCS, the initialization step of the SPT is iterated until online CCS converges to 80%. The number of iterations required for 80% convergence is described in [30] as follows:

$$\mathrm{itr}_{80\%} = \mathrm{ceil}(\mathrm{M}\cdot\mathrm{B}\cdot(\log_{10}(20)-2)/\log_{10}(\eta)) \tag{5}$$

where ceil() denotes the nearest integer above the input value. In the initialization step of the SPT, we consider an additional case in which there exists a peak pair with a harmonic relation.

### C. PROPOSED METHOD

Several subspace methods have been developed to achieve accurate frequency estimation, such as the MUSIC and Blackman-Tukey method. The principal eigenvectors $U = [\mathbf{u}_1 \ldots \mathbf{u}_{\mathrm{P}}]$ of a covariance matrix form the basis of a signal subspace, and the partial pseudospectrum of the Blackman-Tukey method [31], [39] is computed as follows:

$$\mathbf{s}_{\mathrm{BT}} = \frac{1}{\mathrm{P}}\sum_{\mathrm{i}=1}^{\mathrm{P}} \lambda_i \mathrm{F}\mathbf{u}_{\mathrm{i}} \tag{6}$$

where P denotes the number of principal eigenvectors. $\lambda_i$ is the eigenvalue and we assume that $\lambda_i = 1$ for $i = 1{\sim}$P. In this study, we set P as 3. To estimate U, we designed the SST algorithm described in Subsection II-D. The instantaneous HR can be estimated using the SPT with $\mathbf{s}_{\mathrm{BT}}$. Finally, the proposed HR tracking method is constructed by a combination of online CCS, SST, and SPT (see Fig. 1). We denote the proposed HR tracking method as "CCS+SST+SPT".

### D. SIGNAL SUBSPACE TRACKING

There are several methods for estimating the basis of the subspace, such as principal component analysis and various subspace tracking algorithms [40]. Because the principal component analysis requires eigen decomposition with high computational complexity $\mathrm{O}(\mathrm{N}^3\mathrm{B}^3)$, computationally efficient subspace tracking algorithms have been proposed such as the fast Rayleigh's quotient-based adaptive noise subspace (FRANS) [41] and fast data projection method (FDPM) [42]. Based on FRANS and FDPM, we designed a new fast SST algorithm with only the covariance without using the original signal. Similar to FRANS and FDPM, the proposed algorithm maximizes the cost function J to track the signal subspace. We have

$$\mathrm{J} = tr(\Lambda_s) = tr(U^{\mathrm{T}}CU) \tag{7}$$

where $tr()$ denotes the trace of input matrix, $\Lambda_{\mathrm{s}}$ represents the diagonal matrix of eigenvalues for a signal subspace, and $C$ is the covariance matrix in the form of a symmetric Toeplitz matrix, which is transformed from the reconstructed covariance vector $\boldsymbol{c}_k$. We can predict the basis of the signal subspace using gradient of J as follows:

$$\hat{U} = U + \tilde{\mu}\frac{\partial}{\partial U}\mathrm{tr}(U^{\mathrm{T}}CU) \tag{8}$$

where $\tilde{\mu}$ is the normalized value of a step size $\mu$, given as follows:

$$\tilde{\mu} = \mu / |tr(C)| \tag{9}$$

Because the eigenvectors are orthogonal, we orthogonalize $\hat{U}$ using the orthogonalization matrix H of the FRANS [41] as follows:

$$\mathrm{H} = \mathrm{I} - \frac{1}{\tilde{r}}\left(1 - 1\Big/\sqrt{1 + 2\tilde{\mu}\tilde{r} + \tilde{\mu}^2\tilde{c}\tilde{r}}\right)U^{\mathrm{T}}CU \tag{10}$$

where $\tilde{c}$ and $\tilde{r}$ correspond to the power of the signal and sum of the eigenvalues for the signal subspace, respectively. We implemented them as follows:

$$\tilde{c} = tr(C) \tag{11-1}$$

$$\tilde{r} = tr(U^{\mathrm{T}}CU) \tag{11-2}$$

Finally, eigenvectors are normalized. The overall procedure is summarized in Algorithm 2. Although FRANS and FDPM can trace both the signal and noise subspaces, we adopted the signal subspace scheme because it is more stable and robust than the noise subspace tracking scheme.

**Algorithm 2** Fast Signal Subspace Tracking for CCS

**Input:** Recovered covariance matrix $C$ (size: NB $\times$NB)
**Output:** Signal subspace basis $U_k$ (size: NB $\times$P) at iteration $k$

1. Step size normalization
   $\tilde{c} = |tr(C)|$
   $\tilde{\mu} = \mu/\tilde{c}$
2. Gradient ascent optimization
   $\hat{U} = U_{k-1} + \tilde{\mu}CU_{k-1}$
3. Eigenvector orthogonalization
   $\mathrm{R} = U_{k-1}^{\mathrm{T}}CU_{k-1}$
   $\tilde{r} = |tr(\mathrm{R})|$
   $H = \mathrm{I} - \frac{1}{\tilde{r}}\left(1 - 1/\sqrt{1 + 2\tilde{\mu}\tilde{r} + \tilde{\mu}^2\tilde{c}\tilde{r}}\right)\mathrm{R}$
   $\mathrm{Z} = \hat{U}\mathrm{H}$
4. Eigenvector normalization
   $U_k = normalize(\mathrm{Z})$

$\divideontimes$ $tr()$: the trace of an input matrix,
*normalize*(): normalization of the columns of an input matrix

### E. SIMULATION

To evaluate the frequency tracking performance, we considered three simulation types as follows:

$$\mathrm{x[n]} = \mathrm{A}\cos(2\pi\varphi(n)) + \mathrm{wGn}(\sigma^2) \tag{12}$$

$$\dot{\varphi}(\mathrm{n}) = \begin{cases} a. & \beta \\ b. & \alpha \cdot n + \beta \\ c. & \alpha \cdot cos(2\pi\omega n) + \beta \end{cases} \tag{13}$$

where $\alpha$, $\beta$, and $\omega$ are arbitrary constants. $\mathrm{wGn}(\sigma^2)$ denotes a white Gaussian noise with variance $\sigma^2$. The signal-to-noise ratio (SNR) was set to 10 dB. $\dot{\varphi}(n)$ is the derivative of $\varphi(\mathrm{n})$ and is the reference instantaneous HR. The simulation contains three different HR types: a, b, and c corresponding to constant HR, increasing HR, and fluctuating HR, respectively. We adjusted the simulated HR range between 1$\sim$3 Hz. Specifically, the constant HR was assigned as a uniformly distributed random number between 1.5$\sim$2.5 Hz. The starting frequency of the increasing HR was 1 Hz, and the final frequency was a uniform random number between 2$\sim$3 Hz. The amplitude of the fluctuating HR was 0.15 Hz, and its base frequency was a uniformly distributed random number between 1.5$\sim$2.5 Hz. We performed a Monte Carlo simulation with 100 independent simulations for each type of simulation. Each HR tracking performance was evaluated by measuring the error between the reference instantaneous HR and its estimate.

### F. DATA COLLECTION

We used an open-source database (MIT MIMIC database [43]) to evaluate the proposed method and isolated 100 datasets that were less contaminated. PPG and ECG signals were recorded at a sampling rate of 500 Hz for 10 min. The PPG was downsampled to 10 Hz. The R-peaks of the ECG were detected using Pan-Tompkins algorithm [44], and computed the instantaneous reference HR from the interval between successive R-peaks.

## III. RESULTS

The performance of the proposed method was assessed using simulations and real PPG data. For each signal, we calculated the mean absolute error (MAE) between the reference and estimate and excluded the initial 100 samples from the analysis because convergence time is required for the HR tracking algorithms. We evaluated the performance of HR tracking algorithms (ALNF, SPT, CCS+ACNF, CCS+SPT, and proposed CCS+SST+SPT), and searched for their optimal parameters that minimized the MAEs. For multiple comparisons, we performed Kruskal-Wallis test with Bonferroni correction and defined $p < 0.001$ as statistically significant. We used non-parametric Wilcoxon's two-sampled signed-rank test for post hoc analysis. To show the distribution of MAEs, a box plot was used, where the top and bottom boxes represent the 75th and 25th percentiles, and the center, top, and bottom lines are the 50th, 90th, and 10th percentiles, respectively. To calculate the average MAEs, a 10% trimmed mean was used owing to its robustness to outliers.

We considered three simulation types: a. constant HR, b. increasing HR and c. fluctuating HR. Multiple comparisons for the HR tracking algorithms were performed, and there were statistically significant differences for all HR types. Post hoc tests for each simulation type showed that all p-values were less than 0.001 in all comparisons ("ALNF vs. SPT", "ALNF vs. CCS+ACNF", "ALNF vs. CCS+SPT", "ALNF vs. CCS+SST+SPT", "SPT vs. CCS+ACNF", "SPT vs. CCS+SPT", "SPT vs. CCS+SST+SPT", "CCS+ACNF vs. CCS+SPT", "CCS+ACNF vs. CCS+SST+SPT", and "CCS+SPT vs. CCS+SST+SPT"). As shown in Fig. 3, MAEs of "CCS+SST+SPT" were significantly lower than those of "CCS+ACNF", "CCS+SPT", and "CCS+SPT". In time-varying HR simulations (type b and c), MAEs of

**TABLE 1. Average mean absolute errors on real PPG data.**

| ALNF | SPT | CCS +ACNF | CCS +SPT | CCS +SST+SPT |
|---|---|---|---|---|
| 0.7853 beats/min | 1.0348 beats/min | 1.6608 beats/min | 1.4851 beats/min | 1.0425 beats/min |

"CCS+SST+SPT" were significantly lower than those of "SPT".

For real PPG data (see Fig. 4), statistically significant differences were observed in both multiple comparison and post hoc analysis in all comparisons except for "SPT vs. CCS+SST+SPT" (see Fig. 5). MAEs of "CCS+SST+SPT" were significantly lower than those of previous compressed algorithms ("CCS+ACNF" and "CCS+SPT"), and there was no statistically significant difference between the conventional SPT (sampling rate: 10 Hz) and "CCS+SST+SPT" (average sampling rate: 1.4 Hz). The average MAE of the proposed "CCS+SST+SPT" was 1.04 beats/min (see Table 1). Because there is a tradeoff relationship between the estimation accuracy and tracking speed according to the value of $\eta$, we investigated the HR tracking performance for all $\eta$ values at 0.1 intervals, as shown in Fig. 6.

## IV. DISCUSSION

In this study, we proposed a novel HR tracking method that satisfies the requirements of real-time processing, energy-efficient sub-Nyquist sampling, and high accuracy. Sub-Nyquist sampling is the only way to reduce the energy consumption of the active sensor's transmitter, and online CCS is essential for non-stationary signal processing (e.g., time-varying HR tracking). Because the previous HR tracking method based on online CCS showed insufficient accuracy, in this study, we proposed an advanced method comprising online CCS, subspace tracking algorithm, and subspace-based frequency estimation. To the best of our knowledge, this study is the first to report subspace-based frequency tracking with sub-Nyquist sampling. The proposed "CCS+SST+SPT" (average sampling rate: 1.4 Hz) showed better frequency tracking performance than conventional SPT (sampling rate:10 Hz) in time-varying HR simulations, and there was no statistically significant difference between "CCS+SST+SPT" and conventional SPT in real PPG data; the average MAE of "CCS+SST+SPT" was 1.04 beats/min.

The basis for a subspace can be formed by a set of eigenvectors of the covariance matrix, but repetitive eigen decomposition results in huge computational burden. To solve the computational complexity problem, the SST algorithm was designed. Its computational complexity is O(NBP), where P is the dimension of the subspace. Because the dimensions of the signal subspace are much smaller than those of the noise subspace, signal subspace tracking is more efficient. In addition, FRANS is more stable and robust for signal subspace tracking [42]. Hence, we combined the SST algorithm with the online CCS and Blackman-Tukey method.

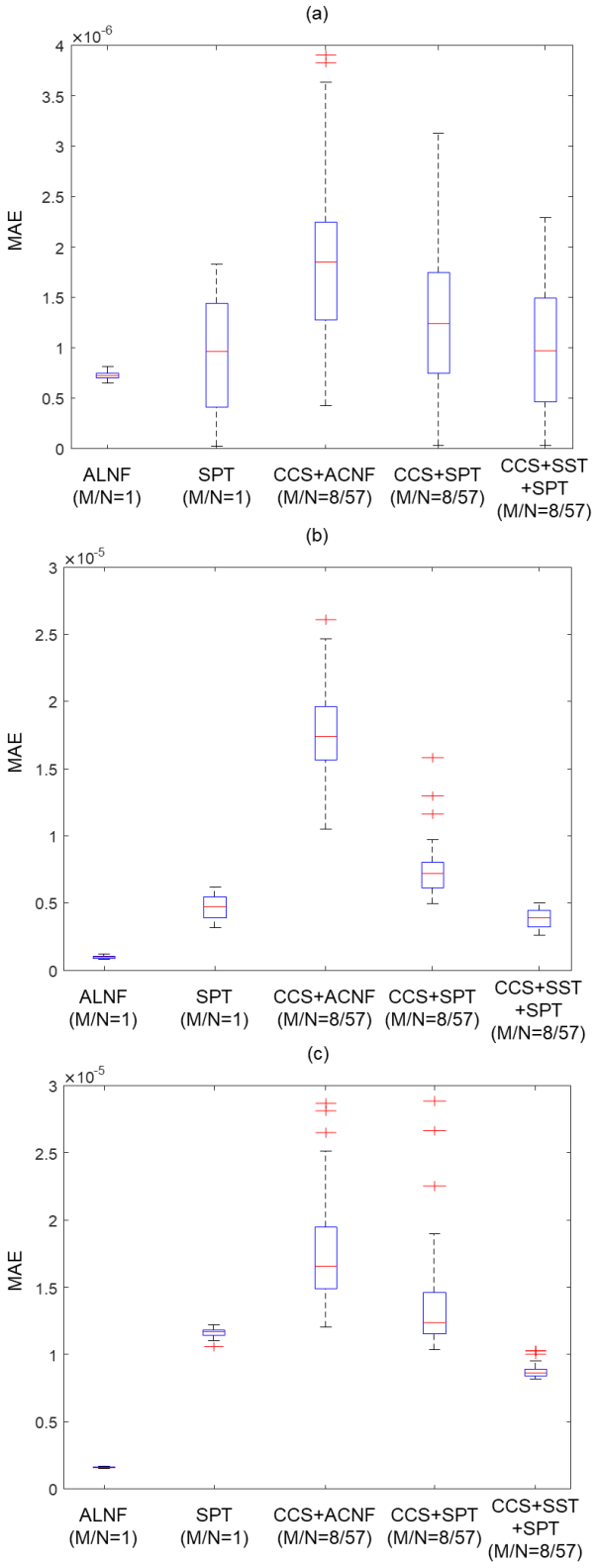


**FIGURE 3. Distribution of MAEs between reference and estimated frequency during simulation. (a) constant HR, (b) increasing HR and (c) fluctuating HR.**

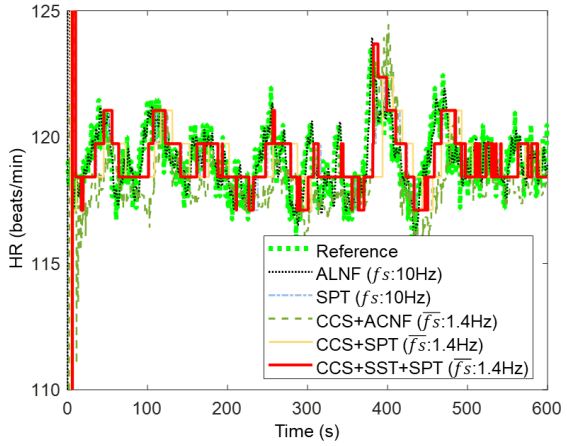


**FIGURE 4.** HR tracking examples. Bold dotted line means the reference HR. Black dotted, blue dash-dotted, green dashed, yellow solid, and red bold lines represent the estimates of ALNF, SPT, CCS+ACNF, CCS+SPT, and CCS+SST+SPT, respectively.

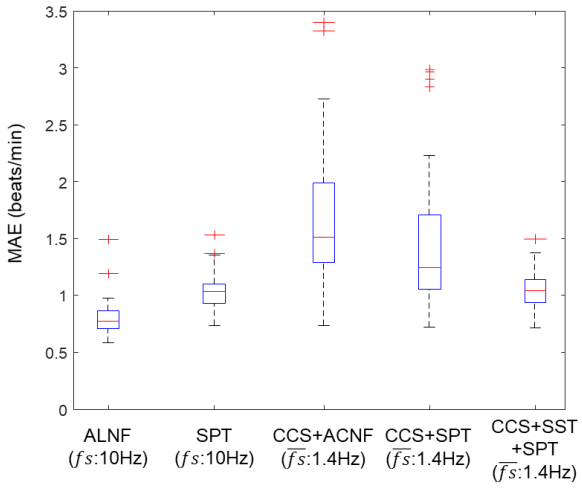


**FIGURE 5.** Distribution of MAEs between reference and estimated HR in real PPG data.

In the proposed method, there is a time lag between the true HR and its estimates (see Fig. 4). Because of the trade-off relationship between accuracy and tracking speed according to $\eta$, it is necessary to adjust the value of $\eta$ according to the degree of non-stationarity of the heart rhythm [30]. We investigated the HR tracking performance according to the value of $\eta$, which determines the tracking speed. As shown in Fig. 6, the "CCS+SST+SPT" was superior to the "CCS+ACNF" and "CCS+SPT" for all values of $\eta$.

The proposed HR tracking method ("CCS+SST+SPT") has several strong points. First, the proposed method dramatically reduces the rate for sampling and LED flashing from 10 Hz to 1.4 Hz. Compared with previous CCS-based HR tracking methods ("CCS+ACNF"), accuracy as well as compressibility (1.8 Hz→1.4 Hz) are significantly improved [19]. Second, its computational complexity, O(NBP·log(NB) + $M^2B^2$), is acceptable. Notably,

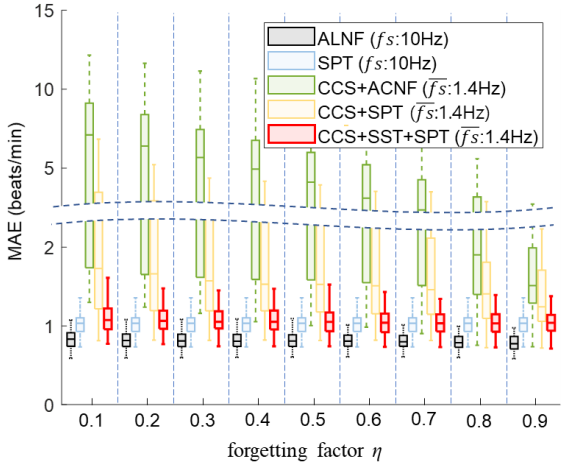


**FIGURE 6.** Trend of MAEs with respect to the value of $\eta$. Dotted black, dash-dotted blue, dashed green, solid yellow, and bold red lines represent the MAEs of ALNF, SPT, CCS+ACNF, CCS+SPT, and CCS+SST+SPT, respectively.

computational efficiency is an important requirement for real-time HR tracking. The computational complexities for the online CCS and Blackman-Tukey methods are O($M^2B^2$) and O(NBP·log(NB)), respectively. If the frequency resolution of the Blackman-Tukey method is improved, its computational complexity will show a quadratic increase. Additionally, the proposed SST has low computational complexity, O(NBP).

Despite the advantages of the proposed method, it has some limitations. First, since the upper and lower peaks of the original PPG cannot be found by sub-Nyquist sampling, the proposed method is not suitable for the conventional algorithms to estimate SpO2 and heart rate variability indices. Nevertheless, these drawbacks might be overcome with the development of advanced algorithms. As specific evidence, the instantaneous HR is related to the tachogram of the heart rate variability analysis [45], and the covariance contains SpO2-related information (AC and DC amplitudes of the PPG) [46]. Second, PPG is easily contaminated by motion artifacts. Since most motion artifacts are within a low frequency band (0.1∼2.5 Hz) [47], [48], aliasing due to motion artifact does not need to be considered but interference in HR estimation should be removed. Unfortunately, the proposed method lacks denoising strategies and outlier tolerance. Although there are several robust subspace tracking algorithms [40], we utilized the FRANS and FDPM schemes owing to their low computational complexities. As shown in Fig. 5., outliers were observed in the estimates of "CCS+SST+SPT" as well as "CCS+ACNF" and "CCS+SPT". Notably, existing signal processing algorithms cannot be directly utilized because the signals acquired by sub-Nyquist sampling are not equispaced. Therefore, it is necessary to develop denoising and robust algorithms. For this reason, we validated the proposed method using only less contaminated MIT-MIMIC data and simulations. Although this study focuses only on HR tracking performance, we plan to generate a new database measured

in various situations to evaluate robustness performance in future works.

## V. CONCLUSION

We propose a novel HR tracking method that consists of online compressive covariance sensing, signal subspace tracking, and spectral peak tracking; The proposed "CCS+SST +SPT" satisfies the requirements of sub-Nyquist sampling, real-time processing, and high accuracy. Its average sampling rate was 1.4 Hz, and averaged absolute error was 1.04 beats/min. We expect that the proposed "CCS+SST+SPT" will be widely used in smart watches and bands. In future work, we will apply it to various applications (e.g., emotion recognition) and develop robust and denoising algorithms for online CCS.

## REFERENCES

[1] A. Guyton and J. Hall, *Textbook of Medical Physiology*, 9th ed. Philadelphia, PA, USA: Elsevier, 1996, doi: 10.4103/sni.sni_327_17.

[2] D. Biswas, N. Simões-Capela, C. Van Hoof, and N. Van Helleputte, "Heart rate estimation from wrist-worn photoplethysmography: A review," *IEEE Sensors J.*, vol. 19, no. 16, pp. 6560–6570, May 2019, doi: 10.1109/JSEN.2019.2914166.

[3] M. A. Motin, C. K. Karmakar, and M. Palaniswami, "Ensemble empirical mode decomposition with principal component analysis: A novel approach for extracting respiratory rate and heart rate from photoplethysmographic signal," *IEEE J. Biomed. Health Inform.*, vol. 22, no. 3, pp. 766–774, May 2018, doi: 10.1109/JBHI.2017.2679108.

[4] M. S. Islam, M. Shifat-E-Rabbi, A. M. A. Dobaie, and M. K. Hasan, "PREHEAT: Precision heart rate monitoring from intense motion artifact corrupted PPG signals using constrained RLS and wavelets," *Biomed. Signal Process. Control*, vol. 38, pp. 212–223, Sep. 2017, doi: 10.1016/J.BSPC.2017.05.010.

[5] Y. S. Yan, C. C. Y. Poon, and Y. T. Zhang, "Reduction of motion artifact in pulse oximetry by smoothed pseudo Wigner-Ville distribution," *J. Neuroeng. Rehabil.*, vol. 2, no. 1, pp. 1–9, Mar. 2005, doi: 10.1186/1743-0003-2-3.

[6] A. Cicone and H. T. Wu, "How nonlinear-type time-frequency analysis can help in sensing instantaneous heart rate and instantaneous respiratory rate from photoplethysmography in a reliable way," *Frontiers Physiol.*, vol. 8, p. 701, Sep. 2017, doi: 10.3389/FPHYS.2017.00701.

[7] C. Park and B. Lee, "Real-time estimation of respiratory rate from a photoplethysmogram using an adaptive lattice notch filter," *Biomed. Eng. OnLine*, vol. 13, no. 1, p. 170, 2014, doi: 10.1186/1475-925X-13-170.

[8] C. Park, H. Shin, and B. Lee, "Blockwise PPG enhancement based on time-variant zero-phase harmonic notch filtering," *Sensors*, vol. 17, no. 4, p. 860, Apr. 2017, doi: 10.3390/s17040860.

[9] N. I. Cho and S. U. Lee, "On the adaptive lattice notch filter for the detection of sinusoids," *IEEE Trans. Circuits Syst. II, Analog Digit. Signal Process.*, vol. 40, no. 7, pp. 405–416, Jul. 1993, doi: 10.1109/82.238368.

[10] Z. Zhang, Z. Pi, and B. Liu, "TROIKA: A general framework for heart rate monitoring using wrist-type photoplethysmographic signals during intensive physical exercise," *IEEE Trans. Biomed. Eng.*, vol. 62, no. 2, pp. 522–531, Feb. 2015, doi: 10.1109/TBME.2014.2359372.

[11] S. H. Fouladi, I. Balasingham, T. A. Ramstad, and K. Kansanen, "Accurate heart rate estimation from camera recording via MUSIC algorithm," in *Proc. 37th Annu. Int. Conf. IEEE Eng. Med. Biol. Soc. (EMBC)*, Aug. 2015, pp. 7454–7457, doi: 10.1109/EMBC.2015.7320115.

[12] I. Kakouche, A. Maali, M. N. El Korso, A. Mesloub, and M. S. Azzaz, "Non-contact measurement of respiration and heart rates based on subspace methods and iterative notch filter using UWB impulse radar," *J. Phys. D, Appl. Phys.*, vol. 55, no. 3, Oct. 2021, Art. no. 035401, doi: 10.1088/1361-6463/AC2C3B.

[13] Z. Zhang, "Photoplethysmography-based heart rate monitoring in physical activities via joint sparse spectrum reconstruction," *IEEE Trans. Biomed. Eng.*, vol. 62, no. 8, pp. 1902–1910, Aug. 2015, doi: 10.1109/TBME.2015.2406332.

[14] T. Schack, C. Sledz, M. Muma, and A. M. Zoubir, "A new method for heart rate monitoring during physical exercise using photoplethysmographic signals," in *Proc. 23rd Eur. Signal Process. Conf. (EUSIPCO)*, Aug. 2015, pp. 2666–2670, doi: 10.1109/EUSIPCO.2015.7362868.

[15] M. Boloursaz Mashhadi, E. Asadi, M. Eskandari, S. Kiani, and F. Marvasti, "Heart rate tracking using wrist-type photoplethysmographic (PPG) signals during physical exercise with simultaneous accelerometry," *IEEE Signal Process. Lett.*, vol. 23, no. 2, pp. 227–231, Feb. 2016, doi: 10.1109/LSP.2015.2509868.

[16] E. Khan, F. Al Hossain, S. Z. Uddin, S. K. Alam, and M. K. Hasan, "A robust heart rate monitoring scheme using photoplethysmographic signals corrupted by intense motion artifacts," *IEEE Trans. Biomed. Eng.*, vol. 63, no. 3, pp. 550–562, Mar. 2016, doi: 10.1109/TBME.2015.2466075.

[17] N. K. L. Murthy, P. C. Madhusudana, P. Suresha, V. Periyasamy, and P. K. Ghosh, "Multiple spectral peak tracking for heart rate monitoring from photoplethysmography signal during intensive physical exercise," *IEEE Signal Process. Lett.*, vol. 22, no. 12, pp. 2391–2395, Dec. 2015, doi: 10.1109/LSP.2015.2486681.

[18] H. Chung, H. Lee, and J. Lee, "Finite state machine framework for instantaneous heart rate validation using wearable photoplethysmography during intensive exercise," *IEEE J. Biomed. Health Inform.*, vol. 23, no. 4, pp. 1595–1606, Jul. 2019, doi: 10.1109/JBHI.2018.2871177.

[19] C. Park and B. Lee, "Energy-efficient photoplethysmogram compression to estimate heart and respiratory rates simultaneously," *IEEE Access*, vol. 7, pp. 71072–71078, 2019, doi: 10.1109/ACCESS.2019.2919745.

[20] D. L. Donoho, "Compressed sensing," *IEEE Trans. Inf. Theory*, vol. 52, no. 4, pp. 1289–1306, Jan. 2006, doi: 10.1109/TIT.2006.871582.

[21] D. Craven, B. McGinley, L. Kilmartin, M. Glavin, and E. Jones, "Compressed sensing for bioelectric signals: A review," *IEEE J. Biomed. Health Inform.*, vol. 19, no. 2, pp. 529–540, Mar. 2015, doi: 10.1109/JBHI.2014.2327194.

[22] M. Mishali and Y. C. Eldar, "From theory to practice: Sub-Nyquist sampling of sparse wideband analog signals," *IEEE J. Sel. Topics Signal Process.*, vol. 4, no. 2, pp. 375–391, Apr. 2010, doi: 10.1109/JSTSP.2010.2042414.

[23] P. Pal and P. P. Vaidyanathan, "Nested arrays: A novel approach to array processing with enhanced degrees of freedom," *IEEE Trans. Signal Process.*, vol. 58, no. 8, pp. 4167–4181, Aug. 2010, doi: 10.1109/TSP.2010.2049264.

[24] C.-L. Liu and P. P. Vaidyanathan, "Super nested arrays: Linear sparse arrays with reduced mutual coupling—Part I: Fundamentals," *IEEE Trans. Signal Process.*, vol. 64, no. 15, pp. 3997–4012, Aug. 2016, doi: 10.1109/TSP.2016.2558159.

[25] J. Liu, Y. Zhang, Y. Lu, S. Ren, and S. Cao, "Augmented nested arrays with enhanced DOF and reduced mutual coupling," *IEEE Trans. Signal Process.*, vol. 65, no. 21, pp. 5549–5563, Nov. 2017, doi: 10.1109/TSP.2017.2736493.

[26] P. P. Vaidyanathan and P. Pal, "Sparse sensing with co-prime samplers and arrays," *IEEE Trans. Signal Process.*, vol. 59, no. 2, pp. 573–586, Feb. 2011, doi: 10.1109/TSP.2010.2089682.

[27] D. Romero, D. D. Arianananda, Z. Tian, and G. Leus, "Compressive covariance sensing: Structure-based compressive sensing beyond sparsity," *IEEE Signal Process. Mag.*, vol. 33, no. 1, pp. 78–93, Jan. 2016. [Online]. Available: http://ieeexplore.ieee.org/abstract/document/7366713/

[28] D. Romero and G. Leus, "Compressive covariance sampling," in *Proc. Inf. Theory Appl. Workshop (ITA)*, Feb. 2013, pp. 1–8, doi: 10.1109/ITA.2013.6502949.

[29] D. Romero, R. Lopez-Valcarce, and G. Leus, "Compression limits for random vectors with linearly parameterized second-order statistics," *IEEE Trans. Inf. Theory*, vol. 61, no. 3, pp. 1410–1425, Mar. 2015. [Online]. Available: http://ieeexplore.ieee.org/abstract/document/7017552/

[30] C. Park and B. Lee, "Online compressive covariance sensing," *Signal Process.*, vol. 162, pp. 1–9, Sep. 2019, doi: 10.1016/J.SIGPRO.2019.04.006.

[31] M. H. Hayes, *Statistical Digital Signal Processing and Modeling*. New York, NY, USA: Wiley, 1996. Accessed: Sep. 2, 2014. [Online]. Available: http://books.google.co.kr/books/about/Statistical_digital_signal_processing_an.html?id=N_VSAAAAMAAJ&pgis=1

[32] G. S. Zavorsky, "Evidence and possible mechanisms of altered maximum heart rate with endurance training and tapering," *Sports Med.*, vol. 29, no. 1, pp. 13–26, Sep. 2000, doi: 10.2165/00007256-200029010-00002.

[33] Z. S. Cicone, C. J. Holmes, M. V. Fedewa, H. V. MacDonald, and M. R. Esco, "Age-based prediction of maximal heart rate in children and adolescents: A systematic review and meta-analysis," *Res. Quart. Exerc. Sport*, vol. 90, no. 3, pp. 417–428, Jul. 2019, doi: 10.1080/02701367.2019.1615605.

[34] J. J. Silverman and O. M. Race, "Paroxysmal tachycardia with a ventricular rate of 365 per minute," *Amer. Heart J.*, vol. 37, no. 7, pp. 1139–1143, Jun. 1949, doi: 10.1016/0002-8703(49)91016-9.

[35] A. Smelin, J. Burstein, H. Blinder, and A. Lubart, "Tachycardia and spontaneous flutter in an adult: Report of a case with rate of 300 and 1:1 flutter," *AMA Arch. Internal Med.*, vol. 91, no. 5, pp. 685–690, May 1953, doi: 10.1001/ARCHINTE.1953.00240170111008.

[36] L. Thuesen, T. Ingemann-Hansen, S. A. Pedersen, I. Jørgensen, N. E. Skakkebaek, and J. S. Christiansen, "Beneficial effects of growth hormone treatment in GH-deficient adults," *Lancet*, vol. 333, no. 8649, pp. 1221–1225, Jun. 1989, doi: 10.1016/S0140-6736(89)92328-3.

[37] L. A. Lisowski, P. M. Verheijen, A. A. Benatar, D. J. G. Soyeur, P. Stoutenbeek, J. I. Brenner, C. S. Kleinman, and E. J. Meijboom, "Atrial flutter in the perinatal age group: Diagnosis, management and outcome," *J. Amer. College Cardiol.*, vol. 35, no. 3, pp. 771–777, Mar. 2000, doi: 10.1016/S0735-1097(99)00589-6.

[38] L. Chhabra, N. Goel, L. Prajapat, D. H. Spodick, and S. Goyal, "Mouse heart rate in a human: Diagnostic mystery of an extreme tachyarrhythmia," *Indian Pacing Electrophysiol. J.*, vol. 12, no. 1, pp. 32–35, Jan. 2012, doi: 10.1016/s0972-6292(16)30463-6.

[39] R. B. Blackman and J. W. Tukey, "The measurement of power spectra from the point of view of communications engineering—Part I," *Bell Syst. Tech. J.*, vol. 37, no. 1, pp. 185–282, Jan. 1958, doi: 10.1002/j.1538-7305.1958.tb03874.x.

[40] N. Vaswani and P. Narayanamurthy, "Static and dynamic robust PCA and matrix completion: A review," *Proc. IEEE*, vol. 106, no. 8, pp. 1359–1379, 2018, doi: 10.1109/JPROC.2018.2844126.

[41] S. Attallah and K. Abed-Meraim, "Low-cost adaptive algorithm for noise subspace estimation," *Electron. Lett.*, vol. 38, no. 12, p. 609, 2002.

[42] X. G. Doukopoulos and G. V. Moustakides, "Fast and stable subspace tracking," *IEEE Trans. Signal Process.*, vol. 56, no. 4, pp. 1452–1465, Apr. 2008, doi: 10.1109/TSP.2007.909335.

[43] A. L. Goldberger, L. A. N. Amaral, L. Glass, J. M. Hausdorff, P. C. Ivanov, R. G. Mark, J. E. Mietus, G. B. Moody, C.-K. Peng, and H. E. Stanley, "PhysioBank, PhysioToolkit, and PhysioNet: Components of a new research resource for complex physiologic signals," *Circulation*, vol. 101, no. 23, pp. e215–e220, Jun. 2000, doi: 10.1161/01.CIR.101.23.e215.

[44] J. Pan and W. J. Tompkins, "A real-time QRS detection algorithm," *IEEE Trans. Biomed. Eng.*, vol. BME-32, no. 3, pp. 230–236, Mar. 1985, doi: 10.1109/TBME.1985.325532.

[45] U. R. Acharya, K. P. Joseph, N. Kannathal, C. M. Lim, and J. S. Suri, "Heart rate variability: A review," *Med. Biol. Eng. Comput.*, vol. 44, no. 12, pp. 1031–1051, Dec. 2006, doi: 10.1007/S11517-006-0119-0.

[46] C. Phillips, D. Liaqat, M. Gabel, and E. de Lara, "Wrist$O_2$: Reliable peripheral oxygen saturation readings from wrist-worn pulse oximeters," in *Proc. IEEE Int. Conf. Pervasive Comput. Commun. Workshops Affiliated Events*, Mar. 2021, pp. 623–629, doi: 10.1109/PERCOMWORKSHOPS51409.2021.9430986.

[47] M. R. Ram, K. V. Madhav, E. H. Krishna, N. R. Komalla, and K. A. Reddy, "A novel approach for motion artifact reduction in PPG signals based on AS-LMS adaptive filter," *IEEE Trans. Instrum. Meas.*, vol. 61, no. 5, pp. 1445–1457, May 2012, doi: 10.1109/TIM.2011.2175832.

[48] H. Han, M.-J. Kim, and J. Kim, "Development of real-time motion artifact reduction algorithm for a wearable photoplethysmography," in *Proc. 29th Annu. Int. Conf. IEEE Eng. Med. Biol. Soc.*, Aug. 2007, pp. 1538–1541, doi: 10.1109/IEMBS.2007.4352596.

**SEUNGYOON NAM** is currently pursuing the Ph.D. degree with the University of Science and Technology (UST), Daejeon, South Korea. He is also involved in research activities with the Emotion Recognition Laboratory, Electronics and Telecommunications Research Institute (ETRI). His research interests include wearable systems for monitoring physiological signal data, emotional computing, biomedical signal processing, emotion recognition using physiological signals, emotional data analysis, and machine learning and artificial intelligence technology related to emotion recognition algorithms.

**CHANKI PARK** received the B.S. degree in control and instrumentation engineering from the Seoul National University of Science and Technology, Seoul, South Korea, and the M.S. and Ph.D. degrees from the School of Mechatronics, Gwangju Institute of Science and Technology (GIST), Gwangju, South Korea. Since 2021, he has been a Senior Researcher with the Electronics and Telecommunications Research Institute (ETRI), Daejeon, South Korea. His current research interests include statistical digital signal processing, biomedical signal processing, affective computing, and machine learning application in medical research areas.

**HYUNSOON SHIN** received the Ph.D. degree in computer science. She is currently the Project Leader with the Brain-Emotional Research Division, Electronics and Telecommunications Research Institute (ETRI), a Professor with the University of Science and Technology (UST), and the President of the Korea Emotion Information and Communication Technology Industry Association (EICT). Her research interests include emotion (brain-emotion), bio-signal and emotion signal processing, wearable device, biomedical signal analysis for human care, physiological emotion recognition algorithm, voice (speech) emotion recognition algorithm, and machine learning and artificial intelligence technology related to emotion recognition algorithms, HX (Human eX) processing, emotional data deep analysis, emotion big data processing, data mining, emotion data knowledge processing, emotion information protocol, and emotional care.